A Catalytic Antibody Programmed for Torsional Activation of Amide Bond Hydrolysis

Ranjana Aggarwal,[a] Fabio Benedetti,*[a] Federico Berti,*[a] Sabrina Buchini,[a] Alfonso Colombatti,[b] Francesca Dinon,[a] Vinicio Galasso,[a] and Stefano Norbedo[a]

Abstract: Amidase antibody 312d6, obtained against the sulfonamide hapten **4a** that mimics the transition state for hydrolysis of a distorted amide, accelerates the hydrolysis of the corresponding amides **1a**–**3a** by a factor of 10^3 at pH 8. The mechanisms of both the uncatalyzed and antibody-catalyzed reactions were studied. Between pH 8 and 12 the uncatalyzed hydrolysis of *N*-toluoylindoles **1a** and **3a** shows a simple first-order dependence on [OH^-], while hydrolysis of **3a** is zeroth-order in [OH^-] below pH 8. The pH profile for hydrolysis of the corresponding tryptophan amide **2a** is more complex due to the dissociation of the zwitterion into an anion with pK_a 9.74; hydrolysis of the zwitterionic and the anionic form of **2a** both show simple first-order dependence on [OH^-]. Absence of ^{18}O exchange between $H_2{}^{18}O/{}^{18}OH^-$ and the substrate, a normal SKIE for both **1a** ($k_H/k_D = 1.12$) and **3a** ($k_H/k_D = 1.24$) and the value of the Hammett constant ρ for hydrolysis of *p*-substituted amides **3a**–**e** are consistent with an ester-like mechanism in which formation of the tetrahedral intermediate is rate-determining and the amine departs as anion. The 312d6-catalyzed hydrolysis of **3a** was studied between pH 7.5 and 9, and its independence of pH in this range indicates that water is the reacting nucleophile. Hydrolysis of **3a** is only partially inhibited by the sulfonamide hapten, and this indicates that non-specific catalysis by the protein accompanies the specific process. Only the nonspecific process is observed in the hydrolysis of amides **3** with *para* substituents other than methyl. Binding studies on the corresponding series of *p*-substituted sulfonamides **5a**–**e** confirm the high specificity of antibody 312d6 for *p*-methyl substituted substrates.

Keywords: amides · catalytic antibodies · heterocycles · hydrolysis · sulfonamides

Introduction

The discovery of antibody catalysis was a major advance in research on artificial enzymes,[1] and provided access to a new class of protein catalysts with enzyme-like properties.[2] Over a hundred catalytic antibodies have been described so far, covering a wide range of reactions and applications, from the asymmetric synthesis of carbon–carbon bonds on the preparative scale[3] to the in vivo activation of prodrugs.[4] Despite this outstanding progress, amide hydrolysis still represents an ambitious target for catalytic antibodies, not only because of the importance of this reaction in nature, but also due to the intrinsic stability of the amide bond. For example, the hydrolysis of unactivated peptides, which is largely dominated by the reaction with water between pH 5 and 9, is exceedingly slow in this pH range, with a half-life of centuries at 37 °C.[5] Hence, an extremely efficient catalyst is needed for the reaction to be even detectable.

Although spontaneous protease activity by auto-antibodies has been demonstrated in several diseases, including haemophylia,[6] only a few antibodies designed to catalyze the hydrolysis of the amide bond have been obtained by the conventional approach based on transition-state analogues. These include anti-phosphonamidate antibody 43C9[7] and polyclonal antiserum PCA 270-29,[8] both of which catalyze the hydrolysis of activated *p*-nitroanilides; primary-amide-hydrolyzing antibodies 13D11[9] and BL25,[10] elicited against a phosphinate and a boronate hapten, respectively; and an amidase antibody that requires an external nucleophilic cofactor.[11] β-Lactamase activity has been described in an antiserum designed for carbonate hydrolysis,[12] and in antibodies obtained by the anti-idiotype approach[13] or by reactive immunization.[14] The intense research effort in this area has also fostered significant progress in the design of transition-state analogues[10, 15] and in the development of new immunization and selection strategies.[14, 16]

[a] Prof. F. Benedetti, Dr. F. Berti, Dr. R. Aggarwal, S. Buchini, F. Dinon, Prof. V. Galasso, Dr. S. Norbedo
Dipartimento di Scienze Chimiche
Università degli Studi di Trieste
Via Giorgieri 1, 34127 Trieste (Italy)
Fax: (+39) 040-558-2402
E-mail: benedett@univ.trieste.it
berti@dsch.univ.trieste.it

[b] Prof. A. Colombatti
Dipartimento di Scienze e Tecnologie Biomediche
Università degli Studi di Udine
P.le Kolbe 4, 33100 Udine (Italy)
Fax: (+39) 0432 494 301

DOI: 10.1002/chem.200204620

With respect to ordinary amides, heterocyclic amides such as *N*-acyl- and *N*-benzoylpyrroles, -indoles and -carbazoles are much more reactive towards hydrolysis due to the aromatic character of the amide nitrogen atom, which lowers the basicity of the amine.[17] We thus chose the hydrolysis of *N*-toluoylindole (**1a**) as model system (Scheme 1) on which to test an approach to hapten design that combines stabilization of the transition state with destabilization of the substrate.

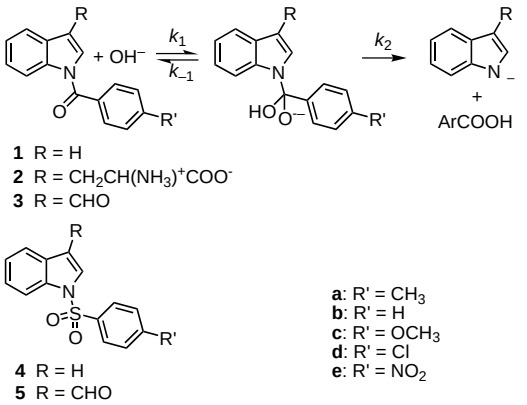

Scheme 1. Hydrolysis of *N*-benzoylindoles and sulfonamide transition-state analogues.

In a previous communication[18] we showed that hydrolysis of amide **1a** (Scheme 1) is accelerated by antibody 312D6, obtained against **4a**, a sulfonamide hapten designed to induce catalysis by transition-state mimicry and torsional activation. We now report full details of the experiments together with new results that indicate that *N*-benzoylindoles **1**–**3** are hydrolyzed with an ester-like mechanism. The results of a study on the effects of substituents R′ on the catalyzed and uncatalyzed reactions and on the binding of sulfonamides **5** are also described and reveal a tight specificity of the antibody for *p*-methyl substituted benzamides.

Results and Discussion

Design and synthesis of the transition-state analogue: In the base-catalyzed hydrolysis of amides, the transition state for the rate-determining addition of hydroxide ion (step 1 of Scheme 1) was shown to be similar to the tetrahedral intermediate.[19] The same holds also for the transition state for breakdown of the same intermediate (step 2), which can be the rate-determining step in the hydrolysis of amides of lower basicity.[17c] Hence, the sulfonamide **4** was selected as hapten to mimic the tetrahedral intermediate and the related transition states.[20]

Calculations indicate that sulfonamides adequately reproduce the geometry and conformation of tetrahedral intermediates for the base-catalyzed hydrolysis of amides, but not the charge distribution.[15e] For this reason, phosphinates[9, 15b] and phosphonamidates,[7, 8, 21] which are ionized at physiological pH, have been preferred as haptens for the generation of amidase antibodies. However, we anticipated that, for the highly reactive amides **1**–**3**, a neutral pathway, corresponding to the uncatalyzed addition of water, might operate at near-neutral pH (see below). We reasoned that a sulfonamide would be a better mimic for the neutral species that are present along this pathway and thus might favour this mechanism in the resulting antibodies.

The second element of design embedded in the structure of the hapten **4** is destabilization of the amide substrate. Twisting the amide group out of planarity reduces amide resonance[22] and increases the reactivity of the carbonyl group towards nucleophiles.[23] Torsional activation of amide hydrolysis, originating from binding the peptide substrate in a distorted, nonplanar conformation, has been suggested to be important in enzyme catalysis,[24] and increased reactivity of twisted amides towards hydrolysis has been demonstrated in model systems.[23, 25] Based on this concept, it was suggested that antibodies raised against a hapten that mimics the structure of a twisted amide should force the substrate to adopt a distorted, more reactive conformation and thus catalyze the reaction by substrate destabilization.[26] This approach was followed by Hansen et al. in the design of conformationally restricted dipeptide analogues in which the peptide bond was replaced by a spiro[4.4]nonyl[26] or cyclobutanol[27] analogue. More recently Gouverneur et al. described the synthesis of a twisted phosphinate hapten, designed to elicit antibodies for the hydrolysis of *N*-benzoylpyrroles.[15b] No antibodies, however, were described by either group.

Figure 1 compares the X-ray crystal structure of *N*-benzenesulfonylindole[28] (**4b**) with the equilibrium structures of the benzamides **1b** and **3b**, optimized with the B3LYP functional[29] and the standard 6-31G(d,p) basis set using the Gaussian 98 suite of programs.[30] The relevant structural parameters are reported in Table 1. In compound **1b** the amide is nearly planar, with the carbonyl group slightly twisted (12°) with respect to the plane of the indole ring, and a twist angle of 38.2° with respect to the plane of the phenyl group. The amide **3b** adopts a similar conformation with more pronounced twists around both the N–C(O) (21.1°) and Ph–C(O) bonds (43.2°). As a consequence, in both amides, the two rings adopt a conformation intermediate between coplanar and bisected, defined by torsion angles ϕ and ψ of 12.3 and 38.0° for **1b** and 21.4 and 43.0° for **3b** (Figure 1, Table 1). In the sulfonamide **4b**, in contrast, a nearly orthogonal conformation with $\phi = 79$ and $\psi = 77°$ is imposed on the rings by the tetrahedral structure of the sulfonyl group.[31] We thus anticipated that antibodies raised against

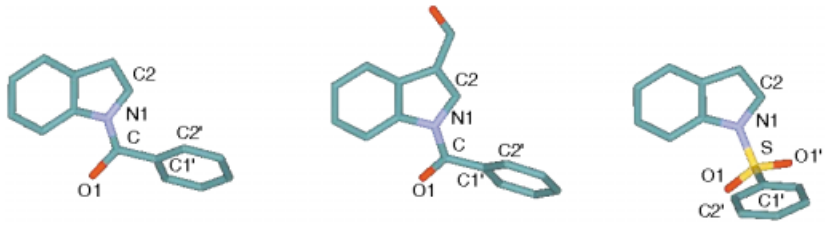

Figure 1. B3LYP/6-31G(d,p) optimized structures of amides **1b** (left) and **3b** (middle) and X-ray crystal structure of sulfonamide **4b** (right).[28]

Table 1. Selected dihedral angles for amides **1b**, **3b** and sulfonamide **4b**.

	1b[a] (X = C)	**3b**[a] (X = C)	**4b**[b] (X = S)
C2-N1-X-O1	−168.0	−158.9	−165.3
C2-N1-X-O1′			−36.1
C2′-C1′-X-O1	−141.8	−136.8	−39.1
ϕ: C2-N1-X-C1′	12.3	21.4	79.0
ψ: N1-X-C1′-C2′	38.0	43.0	77.0

[a] From DFT calculations, this work. [b] From the X-ray crystal structure.[28]

the sulfonamide **4**, on binding the substrates **1**–**3**, would force them to adopt a twisted conformation (Scheme 2) in which the highly distorted amide is expected to be more reactive.

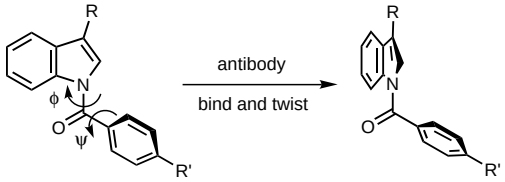

Scheme 2. Torsional activation by antibody 312d6.

Based on this analysis, the p-toluenesulfonamide conjugates **7** and **10** were synthesized (Scheme 3), starting from 3-formylindole. This was converted to the corresponding

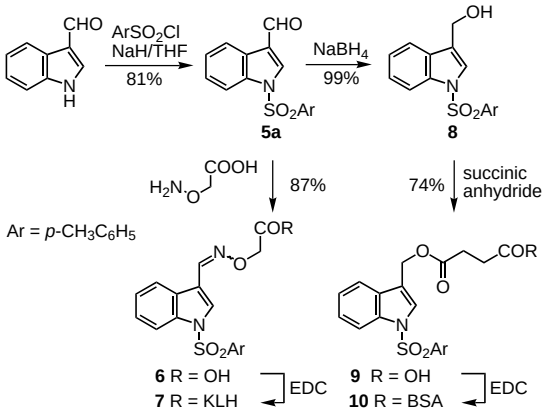

Scheme 3. Synthesis of haptens and conjugates.

anion with NaH in THF and sulfonylated to give the *p*-toluenesulfonamide (**5a**) which, by reaction with *O*-carboxymethylhydroxylamine gave the oxime **6**. Conjugate **7** was obtained by condensation of **6** with keyhole limpet hemocyanin (KLH). Borohydride reduction of the aldehyde **5a** and reaction of the resulting alcohol **8** with succinic anhydride gave the hemisuccinate **9**, which was conjugated to bovine serum albumin (BSA) to give **10**. Both conjugations were carried out by a standard EDC/MES buffer method,[32] and gave two highly modified conjugates that were purified by gel filtration chromatography over Sephadex G-25 and dialysis against water. A spectrophotometric analysis of the conjugate **10** yielded 31 molecules of bound sulfonamide per protein molecule.

Immunization and screening: Three Balb/C mice were immunized with the KLH conjugate **7** by following a standard protocol.[33] After three months and three immunization rounds, the mouse with the highest level of circulating anti-**10** antibodies was sacrificed, and monoclonal antibodies were obtained from its spleen cells. Seventeen binders were selected with an ELISA screening based on binding to the BSA conjugate **10**. Antibodies were purified by immunoaffinity chromatography on protein G and ion-exchange chromatography, and the purified immunoglobulins were assayed for their ability to accelerate the hydrolysis of amide **1a** at pH 7.5 in PBS and at pH 8 in TRIS buffer. Two antibodies showed a significant activity over background, and the most active catalyst, namely, antibody 312D6, an IgG2a, was selected for further characterization and subcloned.

Uncatalyzed hydrolysis of indole amides: Kinetic data for the hydrolysis of amides **1** and **3** were obtained at 25 °C, while the hydrolysis of tryptophan amide **2a** was studied at 37 °C. Faster reactions were followed spectrophotometrically, while slower hydrolyses were monitored by HPLC. All the reactions were run in 10 mM buffer (MES, pH 6–6.5; phosphate, pH 6.5–8; TRIS, pH 8–10; NaOH, pH > 10) containing 10% dioxan, and at constant ionic strength (0.1M NaCl). The observed rate constants for the hydrolysis of amides **1** and **3** were independent of buffer concentration in the range from 0.005 to 0.05 M. For these substrates the uncorrected k_{obs} values were used. In contrast, hydrolysis of the tryptophan amide **2a** shows a significant dependence on the concentration of both phosphate buffer (at pH 7.5) and TRIS buffer in the whole pH range explored. For this substrate the observed rate constants were extrapolated to zero buffer concentration.

The possible general pathways for the base-catalyzed hydrolysis of an amide are shown in Scheme 4. Path a is commonly followed in the hydrolysis of unactivated amides and requires protonation of the amine leaving group by a donor DH. If the basicity of the amine is decreased, path a is disfavoured, and the amine departs as anion via path b and/or path c. In the latter, breakdown of the tetrahedral intermediate is catalyzed by a second hydroxide ion.[17]

Due to the low basicity of indole,[34] path a can be excluded for amides **1**–**3**. A number of studies on the base-catalyzed hydrolysis of amides of indole, and of the related heterocycles pyrrole and carbazole,[17] have shown that these substrates may follow both paths b and c (Scheme 4), the balance between the two being determined by the structure of the substrate and by the medium. To determine the mechanism of the uncatalyzed reactions, we studied the pH dependence of the hydrolysis of amides **1a**, **2a** and **3a**. The corresponding pH profiles are compared in Figure 2. Between pH 8 and 11.5, the hydrolysis of both amides **1a** and **3a** displays a simple first-order dependence on base concentration. The experimental points are well aligned on straight lines with slopes of 0.99 for **1a** and 1.03 for **3a**, and no curvature or inflections due to concurrent processes second-order in [OH^-] can be detected.[17c,f–i)] Path c of Scheme 4 can thus be excluded in favour of path b. The values of k_{obs} between pH 9 and 11.5 were used to calculate the second-order rate constants k_{OH} for the

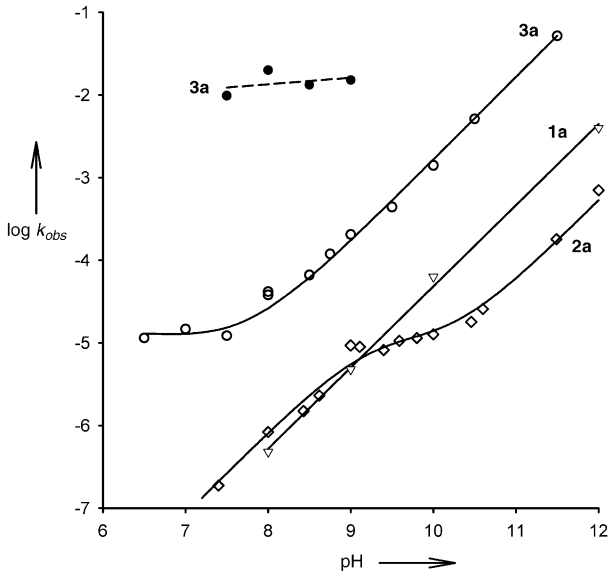

Figure 2. pH–rate profiles for the uncatalyzed hydrolysis of *N*-benzoylindoles **1a** (▽), **2a** (◇) and **3a** (○) and for the 312d6-catalyzed hydrolysis of **3a** (●).

hydroxide-catalyzed processes according to the simple Equation (1).

$$k_{obs} = k_{OH}[OH^-] \quad (1)$$

Values of 0.48 and 16.5 $M^{-1}s^{-1}$ were obtained for **1a** and **3a**, respectively (Table 2).

In the profile for the amide **3a** (Figure 2), a plateau region can be observed below pH 7.5, corresponding to the spontaneous, uncatalyzed hydrolysis of this more reactive substrate. The plateau value gives directly the rate constant for the hydrolysis of **3a** by water ($k_W = 1.30 \times 10^{-5} s^{-1}$).

The pH profile for the hydrolysis of tryptophan amide **2a** is more complex (Figure 2) and can be divided into three regions: below pH 9 and above pH 10.4, a simple first-order dependence on the concentration of hydroxide ion is observed, while in the intermediate region, the behaviour is more complex. The first-order process at higher pH is also intrinsically slower than that at low pH. The discontinuity in the profile can be simply explained with the transition of the amino acid from the zwitterionic form which is present at pH values below its second pK_a, to the anionic form present at higher pH. The profile can be described by a linear combination of the equations for the zwitterionic and anionic forms of the substrate, with the ratio between the two forms as the combination coefficient. This is represented by Equation (2) in which K_W is the dissociation constant of water, k'_{OH} and k''_{OH} are the second-order kinetic constants for the base-catalyzed hydrolysis of the neutral and anionic forms of **2a**, respectively, and pK_{a2} refers to the equilibrium constant for the dissociation of the zwitterion into the anion.

$$\log k_{obs} - \log K_W = \log k''_{OH} + \frac{10^{-(pKa_2 - pH)}}{1 + 10^{-(pKa_2 - pH)}}(\log k'_{OH} - (\log k''_{OH}) + pH \quad (2)$$

Fitting the experimental data to Equation (2) gave values of 0.80 and 0.0421 $M^{-1}s^{-1}$ for the rate constants for hydrolysis of zwitterionic (k'_{OH}) and anionic **2a** (k''_{OH}) (Table 2) and a value of 9.74 for pK_{a2} of tryptophan, in good agreement with literature values.[35] Consistent with classical electrostatic theory, in the base-catalyzed hydrolysis of tryptophan amide **2a**, the anion is more than ten times less reactive than the zwitterion, as a consequence of unfavourable interactions between the reacting anions.

Table 2. Kinetic parameters for the OH^--catalyzed (k_{OH}), uncatalyzed (k_W), and 312d6-catalyzed (k_{cat}, K_M) hydrolysis of indole amides **1a**–**3a**.

Amide	k_{OH} [$M^{-1}s^{-1}$]	$k_W \times 10^5$ [s^{-1}]	$k_{cat} \times 10^5$ [s^{-1}]	K_M [μM]	k_{cat}/k_0	k_{cat}/K_M [$M^{-1}s^{-1}$]
1a[a]	0.48		36	36	>750[e]	10
2a[b,c]	0.80		52	1490	>650[e]	0.35
2a[b,d]	0.0421					
3a[a]	16.5	1.30	1455	160	1120[f]	91

[a] At 298 K. [b] At 310 K. [c] Zwitterion. [d] Anion. [e] Lower limit; for $k_0 = k_{obs}$ at pH 8. [f] $k_0 = k_w$.

Having demonstrated that the hydrolysis of amides **1**–**3** follows the mechanism shown in Scheme 1, corresponding to path b of Scheme 4, it remains to be established whether the rate-limiting step is the formation or the spontaneous breakdown of the tetrahedral intermediate.

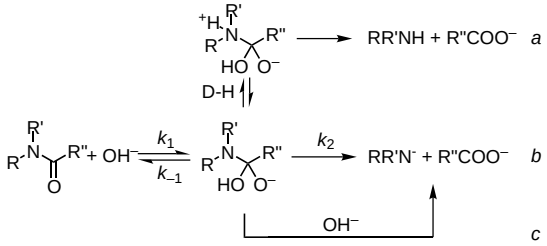

Scheme 4. Mechanisms for the base-catalyzed hydrolysis of amides.

To distinguish between these two possibilities, additional information was obtained from 1) ^{18}O-exchange experiments, 2) D_2O solvent kinetic isotope effect (SKIE: k_H/k_D), and 3) substituent effects in the series of 3-formylindole benzamides **3a**–**e**.

Amides **1a** and **3a** were incubated in 99% $H_2{}^{18}O$ at 25 °C and pH 7.5, and the reaction mixture was analyzed by electrospray mass spectrometry at several time intervals. No measurable ^{18}O incorporation was detected in the unconverted substrates upon incubation for three half-life times for the activated amide **3a** and one half-life time for the less reactive **1a**. In the mechanism shown in Scheme 1, incorporation of ^{18}O in the amide should take place if addition of $^{18}OH^-$ (k_1) is followed by proton equilibration in the tetrahedral intermediate, which is assumed to be fast,[17b] and partitioning of the intermediate between k_2 and expulsion of $^{16}OH^-$ (k_{-1}). The absence of exchange indicates that breakdown of the tetrahedral intermediate to products (k_2) is faster than k_{-1}. Application of the steady-state approximation to the tetrahedral intermediate of Scheme 1 gives Equation (3). If $k_2 \gg k_{-1}$, then Equation (3) simplifies to Equa-

tion (4), that is, formation of the tetrahedral intermediate is the slow step.

$$k_{obs} = \frac{k_1 k_2 [OH^-]}{k_{-1} + k_2} \quad (3)$$

$$k_{obs} = k_1 [OH^-] \quad (4)$$

The hydrolysis of amides **1a** and **3a** was monitored in L_2O (L = H/D), at $[OL^-] = 3.2 \times 10^{-7}$ M (pH 7.5) and 25 °C, where both reactions exhibit normal SKIEs of $k_H/k_D = 1.12$ and 1.24, respectively. In the proposed mechanism (Scheme 1) there are no protons in flight, and thus only a secondary SKIE is expected, due to the reorganization of solvent water molecules around the reacting species. Approximate values of the SKIE for k_1 and k_2 can be calculated by applying an isotopic fractionation analysis[36] to the transition states for the two steps. Figure 3 depicts the structures of the transition states for formation (TS1) and breakdown (TS2) of the tetrahedral

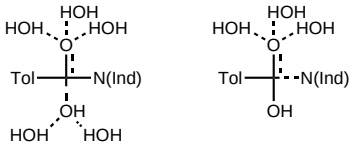

Figure 3. Transition states for formation (TS1) and breakdown (TS2) of the tetrahedral intermediate in the hydrolysis of *N*-toluoylindole.

intermediate with associated water molecules, as proposed by Brown et al. for the hydrolysis of *N*-toluoylpyrrole.[17b] Assuming both transition states to be similar to the tetrahedral intermediate, weighting factors of 0.6 and 0.9 were chosen to describe two limit structures for TS1, corresponding to 60 and 90% advancement along the reaction coordinate, respectively. Similarly, two limit structures for TS2 with 10 and 40% advancement were represented with weighting factors of 0.1 and 0.4. By applying these weighting factors to Gold and Grist's[37] fractionation factors for alkoxide, hydroxide and their solvating water molecules, an approximate SKIE of 0.91 – 1.14 is calculated for k_1, while the corresponding SKIE for k_2 is 0.61 – 0.87. Within the experimental error, the SKIEs measured for the hydrolysis of **1a** ($k_H/k_D = 1.12$) and **3a** ($k_H/k_D = 1.24$) are in good agreement with those predicted for k_1, and support the hypothesis that formation of the tetrahedral intermediate is the slow step.

The hydrolysis of *para*-substituted benzamides **3a**–**e** was monitored at pH 8. The observed rate constants k_{obs} are reported in Table 3, while the Hammett graph obtained by plotting $\log k_{obs}$ against the Hammett constants σ_p for the corresponding substituents is shown in Figure 4a. The experimental points are well aligned on a straight line of slope $\rho = 1.56$ ($r = 0.99$), similar to that obtained by Cipiciani et al. for k_1 (formation of the tetrahedral intermediate) in the closely related hydrolysis of *N*-benzoylpyrroles ($\rho = 1.48$).[17g]

In conclusion, the pH profiles, absence of ^{18}O exchange, secondary SKIE, and Hammett values ρ strongly support the hypothesis that, in base, amides **1**–**3** are hydrolyzed with an

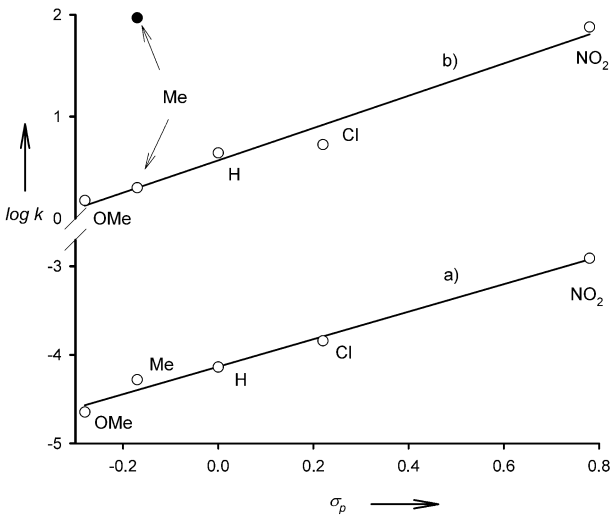

Figure 4. Hammett plots for hydrolysis of amides **3a**–**e** at pH 8 in TRIS buffer. a) uncatalyzed; $k = k_{obs}$. b) 312d6-catalyzed; aspecific catalysis (○): $k = k'_{cat}$; specific catalysis (●): $k = k_{cat}/K_M$.

Table 3. Kinetic parameters for hydrolysis of amides **3a**–**e** in 10% aqueous dioxan at 298 K.

Amide	pH	Uncatalyzed	312d6-catalyzed		
		$k_{obs} \times 10^5$ [s^{-1}][a]	$k_{cat} \times 10^5$ [s^{-1}]	K_M [μM]	k'_{cat} [$M^{-1} s^{-1}$]
3a	7.5	1.53	980	78	1.2
			920[b]	150[b]	
3a	8.0	2.63	1990	170	2.0
3a	8.5	6.18	1330	140	4.7
3a	9.0	17.4	1520	250	13.2
3b	8.0	7.27			4.4
3c	8.0	2.26			1.5
3d	8.0	14.4			5.3
3e	8.0	123			75.7

[a] Observed pseudo-first-order rate constant of the uncatalyzed reaction. [b] FAB fragment.

ester-like mechanism (Scheme 1) in which the rate-determining step is the addition of OH^- to form a tetrahedral intermediate from which the amine departs as anion. This, however, is consistent with the pK_a of the leaving group being comparable to that of a phenol in amide **3** (3-formylindole has a pK_a of 12.4)[38] or to that of an alcohol in substrates **1** and **2**.

The 312d6-catalyzed hydrolysis of indole amides: The 312d6-catalyzed hydrolyses of *N*-toluoylindole (**1a**) and *N*-toluoyltryptophan (**2a**) were monitored at pH 8 in TRIS buffer at 25 and 37 °C, respectively. Both reactions follow saturation kinetics and are reversibly inhibited by the sulfonamide hapten **4a**, a clear indication that the reaction is taking place inside the binding site of the antibody. The rate constants k_{cat} and Michaelis constants K_M were obtained by a standard Lineweaver–Burk treatment of the kinetic data and are reported in Table 2.

The behaviour of the more reactive amide **3a** is more complex. The hydrolysis of this substrate is not completely inhibited by the sulfonamide **4a**, and even in the presence of a 20-fold molar excess of the hapten, a residual acceleration is

present (Figure 5). The uninhibited process can be attributed to nonspecific catalysis by polar groups present outside the binding site, on the protein surface.[39] Partitioning of the observed acceleration between the two catalytic effects thus becomes necessary. The rate of the nonspecific process can be obtained from kinetic experiments run in the presence of 200 μM of inhibitor **4a**, which suppresses the specific catalysis (Figure 5), and the corresponding observed rate constant k'_{cat} is reported in Table 3. The kinetic parameters k_{cat} and K_M for

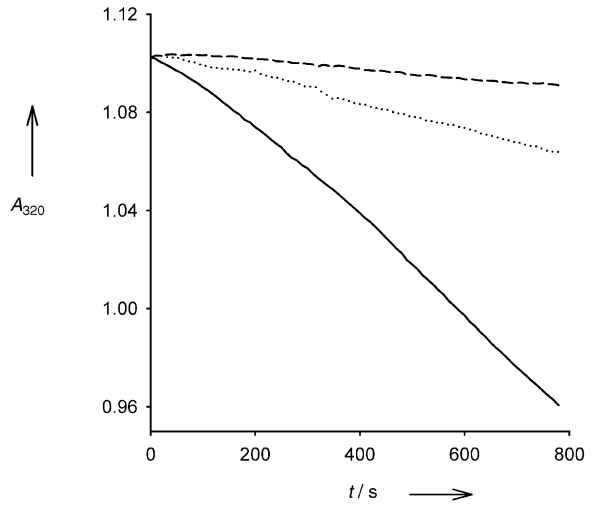

Figure 5. Variation of absorbance at 320 nm for the hydrolysis of amide **3a** (100 μM) in TRIS buffer at pH 8. Dashed line: uncatalyzed reaction. Solid line: with 312d6 (10 μM). Dotted line: with 312d6 (10 μM) and sulfonamide **4a** (200 μM). Approximately 20% of the catalyzed reaction is shown.

the specific process were then obtained from the inhibited fraction of the reaction, which follows the Michaelis–Menten rate law (Figure 6). Similar values of k_{cat} and K_M were obtained for catalysis by the whole antibody and the Fab fragment at pH 7.5 (Table 3). The approach was extended to study the pH dependence of the 312d6-catalyzed hydrolysis of **3a** between pH 7.5 and 9 in TRIS buffer (Table 3 and

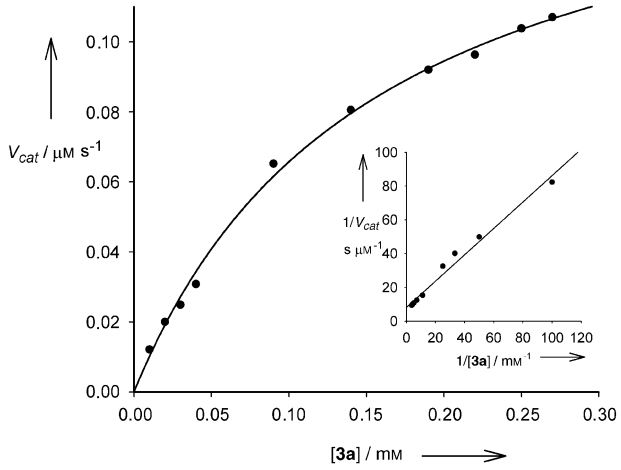

Figure 6. Saturation plot for the specific 312d6-catalyzed hydrolysis of amide **3a** in PBS buffer, pH 7.5. The corresponding Lineweaver–Burk plot is shown in the inset.

Figure 2). Data in Table 3 clearly indicate that the 312d6-catalyzed hydrolysis of indole amide **3a** is pH-independent between pH 7.5 and 9, and a slope of 0.07 was obtained by fitting the experimental points to a straight line (Figure 2). Thus, in the antibody-catalyzed reaction, water is the attacking nucleophile, possibly activated by a general base/acid present in the binding site, which does not change its protonation state in this pH interval. By averaging the experimental values obtained in this pH interval, a value of $1455 \times 10^{-5}\,s^{-1}$ is obtained for k_{cat}, which corresponds to a rate-acceleration factor of 1120 when the rate constant for the spontaneous, pH-independent hydrolysis of amide **3a** ($k_w = 1.3 \times 10^{-5}\,s^{-1}$) is taken as the corresponding uncatalyzed rate constant (Table 2).

For the less reactive amides **1a** and **2a**, spontaneous hydrolysis could not be detected; it is possible, however, to estimate a lower limit for the rate-acceleration factor if the observed pseudo-first-order rate constants for the hydroxide-catalyzed reaction at the same pH are used for the uncatalyzed process. Values of 750 and 650 are thus obtained as lower limits for the rate acceleration factor for the hydrolysis of **1a** and **2a**, respectively (Table 2).

Concentration-dependent inhibition by the sulfonamide **4a** is observed for the hydrolysis of all substrates, as expected for a competitive inhibitor. However, due to the relatively high concentration of antibody required by the kinetic assay (10 μM), it was not possible to obtain a meaningful value of the inhibition constant K_i from kinetic experiments. For this reason the apparent binding constants $K_{d,app}$ of the antibody for hapten **4a** and its 3-formyl derivative **5a** were measured by a competitive ELISA assay[40] and are 1.0 and 1.3 μM for **4a** and **5a**, respectively. Similar values were obtained for the apparent binding constant of the BSA conjugate **10** by a direct ELISA assay[41] (0.86 μM) and by a IAsys resonant mirror experiment[42] (1.4 μM). Considering that analytical methods based on immobilized substrates may overestimate the dissociation constant,[43] it seems safe to assume the value of 1 μM as an upper limit for K_i. For an antibody accelerating a reaction by simple transition-state complementarity, it can been derived that $K_M/K_i = k_{cat}/k_0$.[44] For the 312d6-catalyzed hydrolysis of simple indole amides **1a** and **3a**, by introducing the upper limit of 1 μM for K_i, we obtain for **1a** $K_M/K_i \geq 36$, and for **3a** $K_M/K_i \geq 160$. If we compare these values with the corresponding k_{cat}/k_0 ratios of Table 2, it appears that a substantial fraction of hapten complementarity is reflected in catalytic activity, and this corroborates the choice of sulfonamides as transition-state analogues for the torsionally activated hydrolysis of amides.

The value of the Michaelis constant K_M for tryptophan amide **2a** is more than one order of magnitude higher than the corresponding values observed for amides **1a** and **3a** (Table 2); this may reflect unfavourable electrostatic interactions between the antibody and the charged groups of the amino acid, which are not present in the haptens **4** and **5**.

Antibody 312d6 is not inhibited by the reaction products, as demonstrated by its ability to perform repeated catalytic cycles. In a typical experiment, the antibody was incubated with a 15-fold excess of amide **3a** until hydrolysis of the substrate was complete; a second batch of the same substrate

was then added (again 15-fold excess) and completely hydrolyzed at the same initial rate. The absence of product inhibition indicates that both the *p*-toluoyl residue and the 3-substituted indole ring are essential for recognition by the antibody. This is also confirmed by the tight selectivity displayed by 312d6. The antibody was tested on a number of amides in which the *p*-toluic acid residue was replaced by acetate and cyclohexanecarboxylate, and the indole ring was replaced by another heterocycle (imidazole, carbazole, benzimidazole), none of which was recognized as a substrate.

To further study the specificity of the antibody, the benzamides **3a**–**e** were hydrolyzed at pH 8 in the presence of 312d6. In all cases the reaction was accelerated with respect to background, but only the *p*-tolyl substrate **3a** exhibited clean saturation kinetics; in all the other cases a simple first-order dependence (second-order overall) on the concentrations of antibody and substrate was found. Furthermore, none of the reactions of substrates **3b**–**e** was inhibited by the sulfonamide hapten **4a**, and this indicates that only **3a** is hydrolyzed with a specific mechanism, while the acceleration observed in substrates **3b**–**e** is due to the aspecific effect already noted for **3a**. The (pseudo-)second-order rate constants for the aspecific reactions k'_{cat} (Table 3) were used to construct the Hammett plot of Figure 4b, in which the second-order rate constant k_{cat}/K_M for the specifically catalyzed hydrolysis of **3a** is also reported. All the points for the aspecifically catalyzed reaction lie on a straight line of slope $\rho = 1.56$, identical to that of the uncatalyzed process (1.57). Again it is clear that only in the *p*-methyl-substituted substrate **3a** is the aspecific process accompanied by recognition and specific catalysis.

Binding studies confirm that the absence of specific catalysis in the hydrolysis of amides **3b**–**e** is due to the high specifity of the antibody for *p*-methyl-substituted substrates. Figure 7 reports the results of a competitive ELISA experiment carried out on the series of indole sulfonamides **5a**–**e**, with the same substituents as the corresponding amide substrates **3a**–**e**. In this experiment the free *p*-substituted sulfonamides **5a**–**e** and the immobilized *p*-methylsulfonamide–BSA conjugate **10** were allowed to compete for binding to 312d6. Binding of the antibody to the immobilized sulfonamide was revealed by an anti-mouse IgG conjugated to horseradish peroxidase (HRP), which resulted in an absorption at 450 nm upon incubation with the HRP substrate tetramethylbenzidine (TMB); competition by free sulfonamide results in a decrease in absorption at this wavelength. Figure 7 shows that competition between free *p*-methyl sulfonamide **5a** and bound p-methyl sulfonamide **9** is observed for concentrations of **5a** above 10^{-7} M, while none of the transition state analogues **5b**–**e** competes up to at least 10^{-4} M, that is, on replacing the *p*-methyl substituent with hydrogen, methoxy, chlorine or nitro the affinity for the antibody decreases by a factor of 1000 or more.

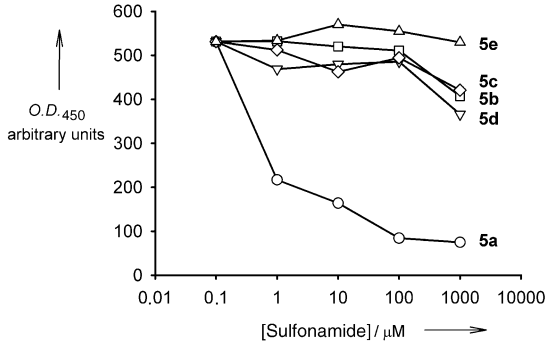

Figure 7. ELISA assay showing binding of 312d6 to *para*-substituted sulfonamides **5a**–**e** in competition with binding to the immobilized hapten–BSA conjugate **10**. Binding to the immobilized hapten was revealed with a secondary anti-mouse IgG conjugated to HRP.

In general, high specificity is common for anti-hapten monoclonal antibodies and is an advantage for analytical applications requiring low cross-reactivity. Conversely, the development of immunoassays with broad specificity may prove surprisingly difficult,[45] and, for catalytic antibodies, special approaches in hapten design and immunization strategy are often required to obtain catalytic species with broad selectivity.[46] In the case of antibody 312d6, which is by no means a strong binder, with a $K_{d,app}$ value for the hapten approaching the μM range, the presence of the methyl group in the *para* position is probably crucial for properly aligning the substrate. Larger groups prevent a correct fit of the molecule in the binding pocket, while smaller groups allow additional freedom for the ligand and hence a loss of binding interactions. In this respect, the behaviour of 312d6 resembles that of antibody 43C9.[7g] This antibody, designed for the hydrolysis of *p*-nitroanilides and esters, failed to display any activity when the *p*-nitro group in the substrate was replaced with a hydrogen atom.

Conclusion

We have demonstrated that cataytic antibodies with amidase activity can be obtained by immunization with a simple, neutral sulfonamide hapten mimicking the transition state for hydrolysis of a twisted amide. The presence of the tetrahedral sulfonyl group and the nearly orthogonal conformation of the indole and benzene rings in the hapten **4** combine to provide in the resulting antibodies transition-state stabilization and substrate destabilization by binding the amide in a nonplanar conformation. Combination of these effects results, in antibody 312d6, in a rate acceleration factor $k_{cat}/k_0 = 10^3$ for the hydrolysis of *N*-(p-methylbenzoyl)indoles **1a**–**3a**. Twisting the amide bond out of planarity can in principle result in very large accelerations.[23a] B3LYP/6-31G(d,p) calculations on model amides **1b** and **3b** indicate that conformations in which the amide bond is twisted by 90° from coplanarity are 8 to 9 kcal mol^{-1} higher in energy with respect to the minimum-energy conformations of Figure 1. Clearly, only a fraction of this energy is expressed as acceleration of the hydrolysis by antibody 312d6. Whether this is due to incomplete twisting of the amide bond by the antibody in the ground state or by unfavourable binding of the transition state remains to be established.

Experimental Section

General: Optical rotations were measured on a Perkin–Elmer 241 polarimeter fitted with a 10 cm cell. IR spectra were recorded using a Thermo-Nicolet FT-IR Avatar 320. ^{1}H and ^{13}C NMR spectra were recorded at 400 and 104 MHz, respectively, on a Jeol EX400 spectrometer, using the residual solvent peak as an internal reference. Chemical shifts are given in parts per million. Coupling constants *J* are given in Hz. EI mass spectra vere measured on a VG 70/70 EIMS spectrometer. ES mass spectra were recorded on a Perkin–Elmer API1 spectrometer. Elemental analyses were recorded on a Carlo Erba EA1110 elemental analyzer. UV/Vis spectra and spectrophotometric kinetic measurements were performed on a Perkin–Elmer Lambda 2 or on a Helios β spectrophotometer. HPLC analyses were run on a Hewlett–Packard 1100 HPLC system. ELISA experiments were always carried out on Nunc maxisorp immunomodules; secondary antibody/HRP conjugates were purchased from Pierce ltd. Plates were washed on an SLT plate washer, and ELISA measurements were obtained on an SLT Spectra Vision microplate reader. THF was freshly redistilled from sodium/benzophenone. Flash column chromatography was performed on silica gel 60H (230–400 mesh) Merck 9385; thin-layer chromatography was performed on silica-coated Merck kieselgel 60F_{254} 0.25 mm plates and visualized by UV irradiation at 254 nm.

General procedure for synthesis of heterocyclic carboxamides: All the heterocyclic amides were synthesized according to ref. [47] The acyl chloride (15 mmol) was slowly added over 20 min with mechanical stirring to a slurry of the heterocyclic compound (10 mmol) and finely powdered sodium hydroxide (1 g) in dry dichloromethane (30 mL) containing Aliquat 337 (40 mg). The mixture was then extracted with 1% aqueous ammonium chloride and water. The organic fraction was dried over anhydrous sodium sulfate, and the solvent was removed. The crude product was then purified by crystallization or by flash chromatography.

1-(4-Methylbenzoyl)indole (1a): 95% from indole and 4-methylbenzoyl chloride; m.p. 95 °C (diisopropyl ether) (lit.: 94 °C[48]) IR (KBr): $\tilde{\nu}$ = 1660 cm^{-1} (C=O); ^{1}H NMR (400 MHz, $CDCl_3$): δ = 2.5 (s, 3H, CH_3), 6.7 (d, 1H, Ind-4),7.31 (m, 1H, Ind-5), 7.33 (d, 2H, Ar),7.35 (d, 1H, Ind-7), 7.38 (m, 1H, Ind-6), 7.60 (d, 1H, Ind-3), 7.66 (d, 2H, Ar), 8.35 (d, 1H, Ind-2); ^{13}C NMR: δ = 21.73, 108.36, 116.43, 120.94, 123.89, 124.89, 127.80, 129.33, 129.52, 130.84, 131.77, 136.14, 142.70, 169.05; EIMS (70 eV): *m*/*z* (%): 235 (20) $[M]^+$, 119 (100) $[p$-MePhCO$]^+$, 91 (35) $[C_7H_7]^+$, 65 (15) $[C_5H_5]^+$; elemental analysis (%) calcd for $C_{16}H_{13}NO$: C 81.7, H 5.56, N 5.95; found: C 81.4, H 5.72, N 5.79.

Benzyl (2*S*)-2-amino-3-[1-(4-methylbenzoyl)indol-3-yl] propanoate: 77% from N^{α}-benzyloxycarbonyl-L-tryptophan benzyl ester and 4-methylbenzoyl chloride; m.p. 129–131 °C, (chloroform/petroleum ether); $[\alpha]_D^{25}$ = −1.31 (*c* = 0.19, DMSO); IR (KBr): $\tilde{\nu}$ = 3400 (NH), 1730 (CO), 1680 cm^{-1} (CO); ^{1}H NMR (400 MHz, [D_6]DMSO): δ = 2.40 (s, 3H, CH_3), 3.03, 3.18 (dd, 1H, *J* = 14.3, 9.6 Hz; dd, 1H, *J* = 14.3, 4.6 Hz; β-CH_2), 4.43 (m, 1H, α-CH), 4.97 (s, 2H, CH_2Ph), 5.10 (s, 2H, CH_2Ph), 7.24–7.45 (m, 16H, Ar and NH), 7.57 (d, 2H, Ar, *J* = 7.9), 7.65 (d, 1H, *J* = 7.51 Hz, Ar), 8.28 (d, 1H, *J* = 8.1 Hz, Ar); ^{13}C NMR: δ = 21.6 (CH_3), 27.9 (β-CH_2), 54.1 (α-CH), 67.0 (CH_2Ph), 67.4 (CH_2Ph), 115.8, 116.4, 118.8, 123.8, 125.2, 125.9, 127.9, 128.1, 128.2, 128.5, 128.6, 129.1, 129.2, 129.4, 130.2, 130.7, 131.5, 134.7, 136.2, 142.6, 155.6 (C=O), 168.3 (C=O), 171.3 (C=O); ESMS *m*/*z* (%): 547 (90) $[M+H]^+$, 564 (48) $[M+NH_4]^+$; elemental analysis (%) calcd for $C_{34}H_{30}N_2O_5$: C 74.71, H 5.53, N 5.12; found: C 73.52, H 5.61, N 4.97.

(2*S*)-2-Amino-3-[1-(4-methylbenzoyl)indol-3-yl]propanoic acid (2a): 80% from benzyl (2*S*)-2-amino-3-[1-(4-methylbenzoyl)indol-3-yl]propanoate by atmospheric-pressure hydrogenation over 5% Pd/C overnight in methanol; m.p. 225–227 °C (ethanol); $[\alpha]_D^{25}$ = −12.50 (*c* = 0.032; DMSO); IR (KBr): $\tilde{\nu}$ = 3700–2000 (OH), 1700, 1650 cm^{-1} (CO); ^{1}H NMR (400 MHz, [D_6]DMSO): δ = 2.35 (s, 3H, CH_3), 2.95 and 3.45 (dd, 1H, *J* = 14.8, 8.6 Hz; dd, 1H, *J* = 14.8, 4.6 Hz; β-CH_2), 4.15 (m, 1H, α-CH), 7.2–7.5 (m, 5H, Ar), 7.71 (d, 2H, *J* = 7.5 Hz, Ar), 8.28 (d, 1 h, *J* = 7.6, Ar); ^{13}C NMR: δ = 21.1 (CH_3), 26.5 (β-CH_2), 53.6 (α-CH), 115.8, 116.7, 119.5, 123.5, 124.6, 126.9, 129.2, 129.4, 130.6, 131.3, 135.9, 142.2, 167.9, 173.5; ESMS *m*/*z* (%): 323 (65) $[M+H]^+$, 361 (63) $[M+K]^+$, 645 (25) $[2M+H]^+$; elemental analysis (%) calcd for $C_{19}H_{18}N_2O_3$: C 70.79, H 5.63, N 8.69; found: C 70.46, H 5.87, N 8.64.

1-(4-Methylbenzoyl)indole-3-carbaldehyde (3a): 92% from indole 3-carbaldehyde and 4-methylbenzoyl chloride in dry THF; m.p. 142–143 °C (ethyl acetate); IR (KBr): $\tilde{\nu}$ = 1705 (C=O), 1672 cm^{-1} (C=O); ^{1}H NMR (400 MHz, CD_3CN): δ = 2.47 (s, 3H, CH_3), 7.43 (m, 2H, Ind-5,6), 7.70 (d, 2H, Ar), 8.15 (s, 1H, Ind-2), 8.22 (d, 1H, Ind-4), 8.28 (d, 1H, Ind-7), 10.0 (s, 1H, CHO); ^{13}C NMR (CD_3CN): δ = 20.8, 116.0, 121.5, 121.6, 125.2, 126.2, 126.3, 129.5, 129.9, 130.3, 136.9, 139.6, 140.1, 168.7, 186.6; EIMS (70 eV): *m*/*z* (%): 263 (35) $[M]^+$, 119 (100) $[ArCO]^+$, 91 (23) $[C_7H_7]^+$; elemental analysis (%) calcd for $C_{17}H_{13}NO_2$: C 77.55, H 4.97, N 5.32; found: C 77.4, H 4.96, N 5.35.

1-Benzoylindole-3-carbaldehyde (3b): 60% from indole-3-carbaldehyde and benzoyl chloride; m.p. 84 °C (diisopropyl ether) (lit.: 83.5 °C[49]); IR (KBr): $\tilde{\nu}$ = 1670 (CO), 1705 cm^{-1} (CO); ^{1}H NMR (400 MHz, $CDCl_3$): δ = 7.3–7.8 (m, 7H, Ind-5,6, Ar), 7.9 (s, 1H, Ind-2), 8.2–8.4 (m, 2H, Ind-4,7), 10.0 (s, 1H, CHO); ^{13}C NMR: δ = 116.1, 122.0, 125.6, 126.6, 128.7, 129.3, 129.4, 130.1, 133.0, 133.5, 136.8, 137.6, 168.5, 185.7; EIMS (70 eV): *m*/*z* (%): 249 (100) $[M]^+$, 144 (25) $[M-PhCO]^+$, 105 (94) $[PhCO]^+$, 77 (53); elemental analysis (%) calcd for $C_{16}H_{11}NO_2$: C 77.10, H 4.45, N 5.62; found: C 77.21, H 4.49, N 5.66.

1-(4-Methoxybenzoyl)indole-3-carbaldehyde (3c): 90% from indole-3-carbaldehyde and 4-methoxybenzoyl chloride; m.p. 95–97 °C (diisopropyl ether); IR (KBr): $\tilde{\nu}$ = 1702, 1685 cm^{-1} (CO); ^{1}H NMR (400 MHz, $CDCl_3$): δ = 3.9 (s, 3H, OCH_3), 7.0–7.1 (dd, 2H, Ar), 7.3–7.4 (m, 2H, Ind-5,6), 7.7–7.8 (dd, 2H, Ar), 8.0 (s, 1H, Ind-2), 8.1–8.2 (m, 1H, Ind-4), 8.3–8.4 (m, 1H, Ind-7), 10.0 (s, 1H, CHO); ^{13}C NMR: δ = 56.3, 115.0, 116.5, 122.4, 122.6, 125.5, 125.9, 126.8, 126.9, 132.7, 137.6, 138.4, 164.3, 168.4, 186.3; EIMS (70 eV): *m*/*z* (%): 279 (50) $[M]^+$, 144 (8) $[M-ArCO]^+$, 136 (75) $[ArCOH]^+$, 135 (100) $[ArCO]^+$; elemental analysis (%) calcd for $C_{17}H_{13}NO_3$: C 73.11, H 4.69, N 5.02; found: C 72.23, H 4.94, N 4.90.

1-(4-Chlorobenzoyl)indole-3-carbaldehyde (3d): 90% from indole-3-carbaldehyde and 4-chlorobenzoyl chloride; m.p. 121–123 °C (petroleum ether/ethyl acetate); IR (KBr): $\tilde{\nu}$ = 1709, 1667 cm^{-1} (CO); ^{1}H NMR (400 MHz, $CDCl_3$): δ = 7.4–7.5 (m, 2H, Ind-5,6), 7.5–7.6 (dd, 2H, Ar), 7.7–7.8 (dd, 2H, Ar), 7.9 (s, 1H, Ind-2), 8.2–8.4 (m, 2H, Ind-4,7), 10.0 (s, 1H, CHO); ^{13}C NMR: δ = 116.0, 122.1, 122.4, 125.6, 126.6, 127.0, 129.4, 130.8, 131.3, 136.7, 137.0, 139.5, 167.3, 185.5; EIMS (70 eV): *m*/*z* (%): 285/283 (10/43) $[M]^+$, 141/139 (30/100) $[p$-ClPhCO$]^+$, 113/111 (7/25) $[p$-ClPh$]^+$; elemental analysis (%) calcd for $C_{16}H_{10}ClNO_2$: C 67.74, H 3.55, N 4.94; found: C 67.83, H 3.59, N 4.87.

1-(4-Nitrobenzoyl)indole-3-carbaldehyde (3e): 65% from indole-3-carbaldehyde and 4-nitrobenzoyl chloride; m.p. 185–188 °C (lit.: 188–190[50]); IR (KBr): $\tilde{\nu}$ = 1705, 1690 cm^{-1} (CO); ^{1}H NMR (400 MHz, [D_6]DMSO): δ = 7.5–7.6 (m, 2H, Ind-5,6), 8.1–8.5 (m, 7H, Ar + Ind), 10.0 (s, 1H, CHO); ^{13}C NMR ([D_6]DMSO): δ = 116.3, 121.6, 123.9, 124.1, 125.8, 126.7, 130.9, 131.0, 136.6, 138.9, 140.5, 150.2, 166.0, 187.5; EIMS (70 eV): *m*/*z* (%): 294 (30) $[M]^+$, 150 (100) $[p$-NO_2PhCO$]^+$, 144 (7) $[M-p$-NO_2PhCO$]^+$, 104 (35) $[C_7H_4O]$; elemental analysis (%) calcd for $C_{16}H_{10}N_2O_4$: C 65.31, H 3.43, N 9.52; found: C 65.77, H 3.39, N 9.98.

General procedure for synthesis of the heterocyclic sulfonamides: All sulfonamides were synthesized by either the procedure described above for the carboxamides (method A), or by the following method B: sodium hydride (35 mmol) was added at room temperature to a solution of indole-3-carbaldehyde (5 g, 35 mmol) in anhydrous THF (200 mL) under an argon atmosphere. After 15 min at room temperature, the sulfonyl chloride (35 mmol) in THF (20 mL) was added. The mixture was heated under reflux for 1 h, cooled, poured into water (100 mL) and extracted with dichloromethane (3 × 100 mL). The organic phases were dried over anhydrous sodium sulfate and evaporated to yield the crude sulfonamide, which was purified by chromatography.

1-[(4-Methylphenyl)sulfonyl]indole-3-carbaldehyde (5a): Method B; 85% from indole-3-carbaldehyde and toluene-4-sulfonyl-chloride; m.p. 149 °C (ethyl acetate) (lit.: 148–150[51]); IR (KBr): $\tilde{\nu}$ = 1160, 1360 (SO_2), 1660 cm^{-1} (CO); ^{1}H NMR (400 MHz, $CDCl_3$): δ = 2.4 (s, 3H, CH_3), 7.26 (d, 2H, Ar), 7.36 (m, 1H, Ind-6), 7.39 (m, 1H, Ind-5), 7.83 (d, 2H, Ar), 7.95 (d, 1H, Ind-4), 8.23 (s, 1H,Ind-2), 8.25 (d, 1H, Ind-7), 10.2 (s, 1H, CHO); ^{13}C NMR: δ = 21.7, 113.3, 122.4, 122.6, 125.1, 126.3, 127.2, 130.3, 134.4, 135.3, 136.2, 146.2, 185.3; EIMS (70 eV): *m*/*z* (%): 299 (38) $[M]^+$, 271 (3), 155 (52) $[ArSO_2]^+$, 139 (3), 116 (14), 91 (100); elemental analysis (%) calcd for $C_{16}H_{13}NSO_3$: C 64.2, H 4.38, N 4.68, S 10.7; found: C 64.1, H 4.35, N 4.58, S 10.6.

1-[(4-Methoxyphenyl)sulfonyl]indole-3-carbaldehyde (5c): method A; 85%; m.p. 137 °C(lit.: 138–140[52]); IR (KBr): $\tilde{\nu}$ = 1150, 1380 (SO_2),

1680 cm^{-1} (CO); ^{1}H NMR (400 MHz, $CDCl_3$): $\delta = 3.8$ (s, 3H, OCH_3), 7.0 (d, 2H, Ar), 7.4 (m, 2H, Ind-5,6), 7.90 (d, 2H, Ar), 7.95 (d, 1H, Ind-5), 8.23 (s, 1H, Ind-2), 8.26 (d, 2H Ind-7), 10.2 (s, 1H, CHO); ^{13}C NMR: $\delta = 55.8$, 113.2, 114.9, 122.2, 122.5, 125.0, 126.2, 128.5, 129.6, 135.1, 136.2, 164.5, 185.3; EIMS (70 eV): *m*/*z* (%): 315 (45) $[M]^+$, 171 (100) $[ArSO_2]^+$, 107 (55) $[C_6H_4OCH_3]^+$; elemental analysis (%) calcd for $C_{16}H_{13}NO_4S$: C 60.94, H 4.16, N 4.44; found: C 62.12, H 4.34, N 4.19.

1-[(4-Chlorophenyl)sulfonyl]indole-3-carbaldehyde (5d): Method A; 78%; m.p. 152–154 °C (ethanol); IR (KBr): $\tilde{\nu} = 1130$, 1370 (SO_2), 1670 cm^{-1} (CO); ^{1}H NMR (400 MHz, $CDCl_3$): $\delta = 7.4$ (m, 2H, Ind-5,6), 7.5 (d, 2H, Ar), 7.9 (d, 2H, Ar), 8.0 (d, 1H, Ind-4), 8.2 (s, 1H, Ind-2), 8.3 (d, 1H, Ind-7), 10.1 (s, 1H, CHO); ^{13}C NMR: $\delta = 113.1$, 122.7, 125.3, 126.3, 126.5, 128.5, 130.0, 135.1, 135.7, 135.8, 141.6, 185.2; EIMS (70 eV): *m*/*z* (%): 321/319 (10/28) $[M]^+$, 177/175 (27/100) $[p\text{-}ClC_6H_4SO_2]^+$, 116 (35), 113/111 (16/65) $[C_6H_4Cl]^+$; elemental analysis (%) calcd for $C_{15}H_{10}NSO_3Cl$: C 56.34, H 3.15, N 4.38; found: C 57.5 H 3.42 N 4.12.

1-[(4-Nitrophenyl)sulfonyl]indole-3-carbaldehyde (5e): 70% from indole-3-carbaldehyde and 4-nitrobenzenesulfonyl chloride; method A (70%) or method B (61%). Yellow crystals from butanol; m.p. 115 °C; IR (KBr): $\tilde{\nu} =$ 1100, 1380 (SO_2), 1380, 1520, (NO_2), 1680 cm^{-1} (CO); ^{1}H NMR (400 MHz, $CDCl_3$): $\delta = 7.40$ (m, 1H, Ind-6), 7.45 (m, 1H, Ind-5), 7.94 (d, 1 h, Ind-4), 8.15 (d, 2H, Ar), 8.20 (s, 1H, Ind-2), 8.26 (d, 1H, Ind-7), 8.35 (d, 2H, Ar), 10.1 (s, 1H, CHO); ^{13}C NMR: $\delta = 34.8$, 62.7, 113.0, 123.0, 124.4, 124.9, 125.4, 127.7, 126.9, 128.1, 128.4, 135.5, 185.0; EIMS (70 eV): *m*/*z* (%): 330 (90) $[M]^+$, 329 (30), 145 (100) $[M - p\text{-}NO_2C_6H_4SO_2]^+$, 144 (50), 116 (75); elemental analysis (%) calcd for $C_{15}H_{10}N_2SO_5$: C 54.6, H 3.05, N 8.48; found: C 54.8, H 3.2, N 8.36.

[((1*E*)-{1-[(4-Methylphenyl)sulfonyl]indol-3-yl}methylene)amino]oxyacetic acid 6: 2N sodium hydroxide (1.1 mL) was added to sulfonamide **5a** (100 mg, 0.33 mmol) and *O*-carboxymethyl hydroxylamine hydrochloride (100 mg, 0.92 mmol) in ethanol (15 mL). The solution was heated at reflux for 1 h, and then concentrated to a final volume of 3 mL. Water (4 mL) was added, and the pH adjusted to 10.5. The solution was extracted with ethyl acetate (2 × 5 mL), acidified with hydrochloric acid to pH 2 and, upon cooling to 4 °C, the crude product precipitated. The yield was 87% after crystallization from water/acetone. M.p. 195.5 (decomp); IR (KBr): $\tilde{\nu} =$ 1160, 1360 (SO_2), 1700 (C=N), 1730 (CO), 2500–3150 cm^{-1} (OH); ^{1}H NMR (400 MHz, [D_6]DMSO): $\delta = 2.35$ (s, 3H, CH_3), 4.8 (s, 2H, CH_2), 7.3–7.7 (m, 4H, Ar+Ind-5,6), 7.8–8.3 (m, 5H, Ar+Ind-4,7), 8.4 (s, 1H, Ind-2), 8.65 (s, 1H); ^{13}C NMR (CD_3COCD_3): $\delta = 21.5$, 71.2, 114.2, 116.5, 124.1, 125.0, 126.5, 127.9, 128.1, 130.4, 131.1, 135.5, 136.5, 145.3, 146.8, 171.0; EIMS (70 eV): *m*/*z* (%): 296 (16) $[M - C_2H_2O_3]^+$, 155 (45) $[ArSO_2]^+$, 142 (6), 114 (5), 91 (100); elemental analysis (%) calcd for $C_{18}H_{16}N_2SO_5$: C 58.1, H 4.33, N 7.52, S 8.61; found: C 58.0, H 4.36, N 7.51, S 8.59.

1-[(4-Methylphenyl)sulfonyl]indol-3-ylmethanol (8): Sodium borohydride (0.54 g, 14 mmol) in water (25 mL) was added dropwise to a solution of sulfonamide **5a** (4 g, 13 mmol) in methanol (50 mL). After 30 min the solution was neutralized with 10% ammonium chloride and extracted with chloroform. The organic phase was dried over anhydrous sodium sulfate, and the solvent evaporated under reduced pressure. The crude oil solidified on wetting with isopropyl ether. 99% Yield after crystallizazion from water/acetone. M.p. 110 °C (lit.: 107 °C[53]); IR (KBr): $\tilde{\nu} = 1175$, 1380 (SO_2), 3400 cm^{-1} (OH); ^{1}H NMR (400 MHz): $\delta = 1.8$ (s, 1H, OH), 2.3 (s, 3H, CH_3), 4.8 (s, 2H, CH_2), 7.8–9.2 (m, 9H); ^{13}C NMR: $\delta = 21.5$, 57.1, 113.7, 119.9, 122.3, 123.3, 123.8, 125, 126.8, 129.4, 129.9, 135.2, 135.4, 145.0; elemental analysis (%) calcd for $C_{16}H_{15}NSO_3$: C 63.8, H 5.02, N 4.65, S 10.6; found: C 63.5, H 4.94, N 4.61, S 10.7.

4-{1-[(4-Methylphenyl)sulfonyl]-1*H*-indol-3-yl}methoxy-4-oxobutanoic acid (9): Sulfonamide **8** (2.5 g, 8.8 mmol) and succinic anhydride (2.62 g, 26 mmol) were heated at reflux in dry pyridine for 4 h. The solvent was evaporated, and the oily residue dissolved in the minimum amount of ethyl acetate. The solution was extracted with 0.5M sulfuric acid, and the aqueous phase discarded. The organic phase was extracted with 0.5% aqueous sodium hydrogencarbonate saturated with sodium carbonate. The basic solution was extracted with ethyl acetate, whereby the organic phase was discarded, then acidified to pH 4 and extracted with ethyl acetate. The organic phase was dried and evaporated to give a brown oil, which was purified by chromatography (chloroform/methanol 95:5). 74% Yield after crystallization from toluene. M.p. 110 °C; IR (KBr): $\tilde{\nu} = 1170$, 1370 (CO), 2800–3400 cm^{-1} (OH); ^{1}H NMR (400 MHz): $\delta = 2.3$ (s, 3H, CH_3), 2.6 (t, 2H, CH_2), 2.7 (t, 2H, CH_2), 5.3 (s, 2H, CH_2), 6.8–8.3 (m, 9H), 10.8 (s, 1H, COOH); ^{13}C NMR: $\delta = 21.6$, 28.9 (2C), 58.2, 113.7, 117.1, 119.7, 123.5, 125.1, 125.7, 126.9, 129.4, 130.0, 135.2 (2C), 145.1, 172.1, 177.6; elemental analysis (%) calcd for $C_{20}H_{19}NSO_6$: C 59.8, H 4.77, N 3.49, S 7.99; found: C 59.3, H 4.74, N 3.44, S 7.98.

KLH conjugate 7: Sulfonamide **6** (1 mg) in 500 µL 0.1M MES buffer at pH 4.5, containing NaCl (0.9M) and DMF (20 vol%), was added to a solution of KLH (2 mg) in 500 µL of milliQ water. EDC (0.5 mg) was added, and the mixture stirred for 2 h at room temperature. The white precipitate was removed by centrifugation, and the solution dialyzed against PBS at 4 °C. The conjugate was purified by gel filtration over G-25, and an apparent value of 210 molecules of bound hapten per molecule of KLH was obtained by spectrophotometric analysis.

BSA conjugate 10: The conjugate was obtained, as described for the immunogenic conjugate **7**, from BSA (2 mg), hemisuccinate **9** (2 mg) and EDC (2 mg). After dialysis and gel filtration, spectrophotometric analysis of the conjugate gave an apparent value of 34 molecules of bound hapten per molecule of BSA.

Immunization and production of monoclonal antibodies: BALB/c mice were immunized with conjugate **7**. 0.1 mg per mouse of protein was emulsified with complete Freund adjuvant and injected intraperitoneally. Four repeated injections every 10–14 d with the same amount of protein emulsified with incomplete Freund adjuvant were administered. Three days after the last booster injection, the spleens were removed and the splenocytes fused with the cell line P3X63Ag8/NS-1.[54] Culture fluids of the resulting hybridomas were screened for anti-**10** activity in ELISA. Seventeen hybridomas that recognized **10** and reacted with the antigens in ELISA assay were selected and subcloned twice before using.

Screening and competition ELISA: The microtitration plates were coated with conjugate **10** diluted in 50 mM carbonate buffer, pH 9.6, to a final concentration of 1 µg per mL. Each microwell was filled with 200 µL of the solution, and the plates were incubated overnight at 4 °C. The wells were washed with 0.05% Tween 20 in PBS buffer, and saturated with 1% gelatin from cold-water fish skin in PBS at 4 °C for 90 min. The same solution was used to prepare all the working solutions of 312d6 (1:80 from ascitic fluids, 1:5 from supernatants) and of the competing haptens. Titrations or competition experiments were performed in a final volume of 200 µL per well at 4 °C for 4 h. After washing, the plates were always incubated with an anti-mouse IgG–HRP conjugate (working dilution 1:10000) for 2.5 h at room temperature. The plates were then washed again, and 100 µL of a 0.1 mg per mL solution of TMB in 100 mM citrate buffer, pH 4, containing 0.01% hydrogen peroxide, was added to each well. The chromogenic reaction was stopped after 30–60 min at room temperature by adding 50 µL of 2M sulfuric acid. The optical density at 450 nm was then read.

Purification of monoclonal antibodies: Purified antibody 312d6, as well as all other antibodies tested in this work, was obtained from the supernatant of the hybridoma cell culture (RPMI Sigma with 15% FCS) and from ascitic fluids. Isolation from large volumes of supernatants started with ammonium sulfate precipitation of the antibody (up to 45% saturation of ammonium sulfate), and was followed by dialysis against PBS buffer and purification on Gamma-bind+ Sepharose (Recombinant Protein G, Pharmacia). Ascitic fluids were loaded directly on the Gamma-bind+ column after filtration and removal of the fatty fraction. The column was washed with PBS buffer until all the unbound proteins were removed, and then the antibody fraction was eluted with 0.5M ammonium acetate, pH 3. The pH was immediately raised to neutral with 1M TRIS pH 9, and then the antibody fractions were dialyzed against 10 mM TRIS, pH 8.5. The Gamma-bind purified antibody fraction was then submitted to further purification on a DEAE-Sepharose Fast Flow ion-exchange column (Pharmacia). The antibody, dissolved in 10 mM TRIS buffer at pH 8.5, was loaded on the column, which was washed with the same buffer. The antibody was then eluted in a gradient of sodium chloride. The antibody thus purified by affinity and ion exchange was finally dialyzed against the kinetic buffer. The purity of the antibody was assessed by SDS-PAGE, and was always >95%. The concentration of antibody was determined either spectrophotometrically or by a bicynchoninic acid (BCA) test using a reference mouse IgG solution for calibration.

Preparation and purification of the Fab fragment of 312d6: 5 mg of antibody 312d6, purified from the ascitic fluids and dialyzed against 100 mM phosphate buffer, pH 7.3, containing EDTA 1.25 mM, was incubated with

50 μg of papain for 6 h at 37 °C. Papain was inactivated by addition of iodoacetamide, and the Fab fragment was purified by ion exchange chromatography over DEAE/Trisacryl + M at pH 7.5 (phosphate), and then by gel filtration over sephacryl S-100 HR.

Kinetics of uncatalyzed reactions: The hydrolyses were monitored spectrophotometrically at 25 ± 0.1 °C (amides **1a**, **3**) or at 37 ± 0.1 °C (amide **2a**). Preliminary scans of the whole UV spectrum showed that all the reactions were accompanied by a significant spectral change, with at least two isosbestic points being always present. Reactions were monitored at the wavelength corresponding to the maximum spectral change, that is, 320 nm for **1a**, **3a**, **3c**, **3d**, 310 nm for **2a** and **3b** and 340 nm for **3e**. All the measurements were performed under pseudo-first-order conditions: 50 μL of a 1 mM mother solution of the substrates in dioxane (DMSO for **2a**) were added to 450 μL of 10 mM buffer containing 100 mM NaCl. The final substrate concentration was always 10^{-4} M, with the exception of poorly soluble **3e**, which was used at 5×10^{-5} M. Reactions were followed in most cases for at least three half-life times, and all the measurements were triplicated. Rate constants were obtained by plotting $\log(A - A_\infty)$ versus time; the Guggenheim method[55] was used for the slowest reactions (**1a** and **2a** at pH 7–8). Hydrolysis of **1a** was also monitored by HPLC/fluorescence: 100 μL aliquots of the **1a** solutions were drawn at time intervals and mixed with 100 μL of a 50 μM aqueous solution of the internal standard 3-hydroxymethylindole. The samples were analyzed on an Alltech Alltima C18 250 × 4.6 mm column with water/acetonitrile (50:50) as mobile phase at a flow rate of 1 mL min^{-1}. The fluorescence detector was set to an excitation wavelength of 270 nm, while the emission was read at 343 nm. The retention times are 6.5 min for the internal standard, and 12 min for indole.

Kinetic measurements in the presence of antibodies: The concentration of antibody was usually set to 5–10 μM by dilution of stock solutions of purified antibody. Aliquots of stock solutions of substrates in the organic solvent were added to a final volume of 500 μL containing 10% of the organic solvent. The concentration of the substrates ranged from 5 to 250 μM, depending on solubility. Reactions were monitored spectrophotometrically at the same wavelengths used for the uncatalyzed reactions, or by HPLC for **1a**. The observed initial rates for the first 5% of reaction were obtained from the slopes of plots of the concentration of substrate versus time. The initial rates of the catalyzed reactions were corrected for the background reaction. Hydrolyses of the substrates were always monitored for the whole reaction to verify that the overall spectral change corresponded to the complete conversion to products.

Acknowledgements

This work was supported by the CNR (Progetto Finalizzato Biotecnologie) and by the European Union (contract ERB FMRX-CT98-0193). S.N. thanks the Centre of Excellence for Biocrystallography of the University of Trieste for a postdoctoral grant. R.A. thanks CIB for a grant. We are grateful to Dr. Fabio Hollan for mass spectra, and to Dr. Benoît Gigant, Laboratoire d'Enzymologie et Biochimie Structurales, CNRS, Gif sur Yvette, for setting up the conditions of the papain digestion. We are grateful to Thermo Labsystems and to Dr. Roberta Collino for IASYS affinity measurements.

[1] a) A. J. Kirby, *Angew. Chem.* **1996**, *108*, 770–790; *Angew. Chem. Int. Ed.* **1996**, *35*, 707–724; b) W. B. Motherwell, M. J. Bingham, Y. Six, *Tetrahedron* **2001**, *57*, 4663–4686.

[2] a) D. N. Bolon, C. A. Voigt, S. L. Mayo, *Curr. Opin. Chem. Biol.* **2002**, *6*, 125–129; b) D. Hilvert, *Annu. Rev. Biochem.* **2000**, *69*, 751–793; c) G. M. Blackburn, A. Garçon, *Biotechnology*, 2nd ed., *Vol. 8b* (Ed.: D. R. Kelly), Wiley-VCH, Weinheim, **2000**, pp. 404–490; d) J. D. Stevenson, N. R. Thomas, *Nat. Prod. Rep.* **2000**, *17*, 535–577; e) J. L. Reymond, *Top. Curr. Chem.* **1999**, *200*, 59–93.

[3] S. C. Sinha, J. Sun, G. P. Miller, M. Wartmann, R. A. Lerner, *Chem. Eur. J.* **2001**, *7*, 1691–1702.

[4] C. Rader, B. List, *Chem. Eur. J.* **2000**, *6*, 2091–2095

[5] a) R. M. Smith, D. E. Hansen, *J. Am. Chem. Soc.* **1998**, *120*, 8910–8913; b) R. A. R. Bryant, D. E. Hansen, *J. Am. Chem. Soc.* **1996**, *118*, 5498–5499; c) A. Radzicka, R. Wolfended, *J. Am. Chem. Soc.* **1996**, *118*, 6105–6109; d) H. Slebocka-Tilk, R. S. Brown, *J. Org. Chem.* **1987**, *52*, 805–808.

[6] S. Lacroix-Desmazes, J. Bayry, N. Misra, M. P. Horn, S. Villard, A. Pashov, N. Stieltjes, R. d'Oiron, J. Saint-Remy, J. Hoebeke, M. D. Kazatchkine, S. V. Kaveri, *New Engl. J. Med.* **2002**, *346*, 662–667.

[7] a) K. D. Janda, D. Schloeder, S. J. Benkovic, R. A. Lerner, *Science* **1988**, *241*, 1188–1191; b) S. J. Benkovic, J. A. Adams, C. L. Borders, Jr., K. D. Janda, R. A. Lerner, *Science* **1990**, *250*, 1135–1139; c) K. D. Janda, A. Ashley, T. M. Jones, *J. Am. Chem. Soc.* **1990**, *112*, 8886–8888; d) L. J. Liotta, P. A. Benkovic, G. P. Miller, S. J. Benkovic, *J. Am. Chem. Soc.* **1993**, *115*, 350–351; e) J. D. Stewart, V. A. Roberts, N. R. Thomas, E. D. Getzoff, S. J. Benkovic, *Biochemistry* **1994**, *33*, 1994–2003; f) M. M. Tayer, E. H. Olender, A. S. Arvai, C. K. Koike, I. L. Canestrelli, J. D. Stewart, S. J. Benkovic, E. D. Getzoff, V. A. Roberts, *J. Mol. Biol.* **1999**, *291*, 329–345; g) R. A. Gibbs, P. A. Benkovic, K. D. Janda, R. A. Lerner, S. J. Benkovic, *J. Am. Chem. Soc.* **1992**, *114*, 3528–3534.

[8] G. Gallacher, M. Searcey, C. S. Jackson, K. Brocklehurst, *Biochem. J.* **1992**, *284*, 675–680.

[9] M. T. Martin, T. S. Angeles, R. Sugasawara, N. I. Aman, A. D. Napper, M. D. Darsley, R. I. Sanchez, P. Booth, R. C. Titmas, *J. Am. Chem. Soc.* **1994**, *116*, 6508–6512.

[10] C. S. Gao, B. J. Lavey, C. H. L. Lo, A. Datta, P. Wentworth, K. D. Janda, *J. Am. Chem. Soc.* **1998**, *120*, 2211–2217.

[11] O. Ersoy, R. Fleck, A. Sinskey, S. Masamune, *J. Am. Chem. Soc.* **1998**, *120*, 817–818.

[12] E. L. Ostler, M. Resmini, G. Boucher, N. Romanov, K. Brocklehurst, G. Gallacher, *Chem. Commun.* **2002**, 226–227.

[13] a) H. Debat, B. Avalle, O. Chose, C. O. Sarde, A. Friboulet, D. Thomas, *FASEB J.* **2001**, *15*, 815–822; b) B. Avalle, H. Debat, A. Friboulet, D. Thomas, *Appl. Biochem. Biotechnol.* **2000**, *83*, 163–171; c) B. Avalle, D. Thomas, A. Friboulet, *FASEB J.* **1998**, *12*, 1055–1060.

[14] F. Tanaka, H. Almer, R. A. Lerner, C. F. Barbas III, *Tetrahedron Lett.* **1999**, *40*, 8063–8066.

[15] a) D. J. Tantillo, K. N. Houk, *Chem. Biol.* **2001**, *8*, 535–545; b) M. Schuman, X. Lopez, M. Karplus, V. Gouverneur, *Tetrahedron* **2001**, *57*, 10299–10307; c) C. Jimenez, A. Tramontano, *Tetrahedron Lett.* **2001**, *42*, 7819–7822; d) O. Ersoy, R. Fleck, M. J. Blanco, S. Masamune, *Bioorg. Med. Chem.* **1999**, *7*, 279–286; e) J. L. Radkiewicz, M. A. McAllister, E. Goldstein, K. N. Houk, *J. Org. Chem.* **1998**, *63*, 1419–1428.

[16] a) P. Wentworth, *Science* **2002**, *296*, 2247–2249; b) T. Tsumuraya, H. Suga, S. Meguro, A. Tsunukawa, S. Masamune, *J. Am. Chem. Soc.* **1995**, *117*, 11390–11396; c) O. Ersoy, R. Fleck, A. Sinskey, S. Masamune, *J. Am. Chem. Soc.* **1996**, *118*, 13077–13078.

[17] a) B. Y. Liu, R. S. Brown, *J. Org. Chem.* **1993**, *58*, 732–734; b) R. S. Brown, A. J. Bennett, H. Slebocka-Tilk, *Acc. Chem. Res.* **1992**, *25*, 481–488; c) R. S. Brown, A. J. Bennett, H. Slebocka-Tilk, A. Jodhan, *J. Am. Chem. Soc.* **1992**, *114*, 3088–3092; d) H. Slebocka-Tilk, A. J. Bennett, H. S. Hogg, R. S. Brown, *J. Am. Chem. Soc.* **1991**, *113*, 1288–1294; e) H. Slebocka-Tilk, A. J. Bennett, J. W. Keiller, R. S. Brown, J. P. Guthrie, A. Jodhan, *J. Am. Chem. Soc.* **1990**, *112*, 8507–8514; f) P. Linda, A. Stener, A. Cipiciani, G. Savelli, *J. Heterocycl. Chem.* **1983**, *20*, 247–248; g) A. Cipiciani, P. Linda, G. Savelli, *J. Heterocycl. Chem.* **1979**, *16*, 673–676; h) A. Cipiciani, P. Linda, G. Savelli, *J. Heterocycl. Chem.* **1979**, *16*, 677–678; i) F. M. Menger, J. A. Donohue, *J. Am. Chem. Soc.* **1973**, *95*, 432–437.

[18] F. Benedetti, F. Berti, A. Colombatti, C. Ebert, P. Linda, F. Tonizzo, *Chem. Commun.* **1996**, 1417–1418.

[19] M. Štrajbl, J. Florian, A. Warshel, *J. Am. Chem. Soc.* **2000**, *122*, 5354–5366, and references therein.

[20] Another example of a sulfonamide hapten for the generation of amidase antibodies is reported in ref. [15c]. However, antibodies were not described.

[21] L. J. Liotta, P. A. Benkovic, G. P. Miller, S. J. Benkovic, *J. Am. Chem. Soc.* **1993**, *115*, 350–351.

[22] a) A. J. Kirby, I. V. Komarov, K. Kowski, P. Rademacher, *J. Chem. Soc. Perkin Trans. 2* **1999**, 1313–1316; b) N. H. Werstiuk, R. S. Brown, Q. Wang, *Can. J. Chem.* **1996**, *74*, 524–532; c) A. Greenberg, C. A. Venanzi, *J. Am. Chem. Soc.* **1993**, *115*, 6951–6957; d) A. J. Bennet, V.

Somayaji, R. S. Brown, B. D. Santarsiero, *J. Am. Chem. Soc.* **1991**, *113*, 7563 – 7571.
[23] a) A. J. Kirby, I. V. Komarov, N. Feeder, *J. Chem. Soc. Perkin Trans. 2* **2001**, 522 – 529; b) G. M. Blackburn, C. J. Skaife, I. T. Kay, *J. Chem. Res. (M)* **1980**, 3650 – 3669.
[24] W. P. Jencks, *Catalysis in Chemistry and Enzymology*, McGraw-Hill, New York, **1969**.
[25] a) J. P. Lee, R. Bembi, T. H. Fife, *J. Org. Chem.* **1997**, *62*, 2872 – 2876; b) V. Somayaji, R. S. Brown, *J. Org. Chem.* **1986**, *51*, 2676 – 2686.
[26] P. Yuan, R. Plourde, M. R. Shoemaker, C. L. Moore, D. E. Hansen, *J. Org. Chem.* **1995**, *60*, 5360 – 5364.
[27] P. Yuan, M. R. Driscoll, S. J. Raymond, D. E. Hansen, R. A. Blatchly, *Tetrahedron Lett.* **1994**, *35*, 6195 – 6198.
[28] R. L. Beddoes, L. Dalton, J. A. Joule, O. S. Mills, J. D. Street, C. Watt, F. Ian, *J. Chem. Soc. Perkin Trans. 2* **1986**, 787 – 798.
[29] A. D. Becke, *J. Chem. Phys.* **1993**, *98*, 5648 – 5652.
[30] Gaussian 98, Revision A6M, J. Frisch, G. W. Trucks, H. B. Schlegel, G. E. Scuseria, M. A. Robb, J. R. Cheeseman, V. G. Zagrzewski, J. A. Montgomery, R. E. Stratmann, J. C. Burant, S. Dapprich, J. M. Millam, A. D. Daniels, K. N. Kudin, M. C. Strain, O. Farkas, J. Tomasi, V. Barone, M. Cossi, R. Cammi, B. Mennucci, C. Pomelli, C. Adamo, S. Clifford, J. Ochterski, G. A. Petersson, P. Y. Ayala, Q. Cui, K. Morokuma, D. K. Mailck, A. D. Rabuck, K. Raghavachari, J. B. Foresman, J. Cioslowski, J. V. Ortiz, B. B. Stefanov, G. Liu, A. Liashenko, P. Piskorz, I. Komaromi, R. Gomperts, R. L. Martin, D. J. Fox, T. Keith, M. A. Al-Laham, C. Y. Peng, A. Nanyakkara, C. Gonzales, M. Challacombe, P. M. W. Gill, B. G. Johnson, W. Chen, M. W. Wong, J. L. Andres, M. Head-Gordon, J. A. Pople, Gaussian Inc., Pittsburgh, PA, **1998**.
[31] Semiempirical (PM3) calculations confirm that this is the preferred conformation also in the gas phase.
[32] G. T. Hermanson in *Bioconjugates Techniques*, Academic Press, San Diego, **1995**, pp. 429 – 436.
[33] E. Harlow, D. Lane in *Antibodies, a Laboratory Manual*, Cold Spring Harbor Laboratory, Cold Spring Harbor, **1988**, pp. 139 – 243.
[34] Values of -0.44 and -0.98 were measured for the pK_a of protonated indole: a) G. Reddy, S. Satyanarayana, K. Veera Reddy, *Ind. J. Chem. Sect. A* **1989**, *28*, 337 – 339; b) N. Emanuel, P. K. Battacharya, *J. Ind. Chem. Soc.* **1985**, *62*, 940 – 944.
[35] a) D. V. Jahagirdar, B. R. Arbad, T. K. Chondhekar, S. U. Pakanti, *Ind. J. Chem. Sect. A* **1989**, *28*, 366 – 370; b) R. F. Jameson, G. Hunter, T. Kiss, *J. Chem. Soc. Perkin Trans. 2* **1980**, 1105 – 1110.
[36] a) R. L. Schowen, *Prog. Phys. Org. Chem.* **1972**, *9*, 275 – 332; b) K. B. J. Schowen in *Transition States of Biochemical Processes* (Eds.: R. D. Gandour, R. L. Schowen), Plenum Press, New York, **1978**, pp. 225 – 283.
[37] V. Gold, S. Grist, *J. Chem. Soc. Perkin Trans. 2* **1972**, 89 – 95.
[38] F. Terrier, F. Millot, R. Schaal, *Bull. Soc. Chim. Fr.* **1969**, *9*, 3002 – 3007.
[39] A. J. Kirby, F. Hollfelder, D. Tawfik, *Appl. Biochem. Biotechnol.* **2000**, *83*, 173 – 180.
[40] B. Friguet, A. F. Chaffotte, C. Djaudi-Ohaniance, M. E. Goldberg, *J. Immunol. Meth.* **1985**, *77*, 315.
[41] E. E. M. G. Loomans, A. J. M. Roelen, H. S. Van Damme, H. P. J. Bloemers, T. C. J. Gribman, W. J. G. Schielen, *J. Immunol. Meth.* **1995**, *184*, 207 – 217.
[42] a) R. Cush, J. M. Cronin, W. J. Stewart, C. H. Maule, J. Molloy, N. J. Goddard, *Biosensors Bioelectron.* **1993**, *8*, 347 – 353; b) P. E. Buckle, R. D. Davies, T. Kinning, D. Yeung, P. R. Edwards, D. Pollard-Knight, C. R. Lowe, *Biosensors Bioelectron.* **1993**, *8*, 355 – 363.
[43] a) M. Stenberg, H. Nygren, *J. Immunol. Methods* **1988**, *113*, 3 – 15; b) A. Azimzadeh, J. L. Pellequer, M. H. V. Van Regenmortel, *J. Mol. Recognit.* **1992**, *5*, 9 – 17; c) J. L. Pellequer, M. H. V. Van Regenmortel, *J. Immunol. Meth.* **1993**, *166*, 133 – 143.
[44] J. D. Stewart, S. J. Benkovic, *Nature* **1995**, *375*, 388 – 391.
[45] C. A. Spinks, G. M. Wyatt, S. Everest, R. Jackmann, M. R. A. Morgan, *J. Sci. Food Agricol.* **2002**, *82*, 428 – 434.
[46] a) S. Kurihara, T. Tsumuraya, K. Suzuki, M. Kuroda, L. D. Liu, Y. Takaoka, I. Fujii, *Chem. Eur. J.* **2000**, *6*, 1656 – 1662; b) A. I. Khalaf, S. Linaza, A. R. Pitt, W. H. Stimson, C. J. Suckling, *Tetrahedron* **2000**, *56*, 489 – 495; c) Y. Wada, M. Ono, *J. Prot. Chem.* **1999**, *18*, 199 – 204; d) B. Gigant, J. B. Charbonnier, Z. Eshar, B. S. Green, M. Knossow, *J. Mol. Biol.* **1998**, *284*, 741 – 750; e) C. H. L. Lo, C. S. Gao, S. L. Mao, K. Matsui, R. A. Lerner, K. D. Janda, *Isr. J. Chem.* **1996**, *36*, 195 – 198; f) F. Tanaka, K. Kinoshita, R. Tanimura, I. Fujii, *J. Am. Chem. Soc.* **1996**, *118*, 2332 – 2339.
[47] V. O. Illi, *Synthesis* **1979**, 387 – 390.
[48] P. Bourgeois, J. Mesdoure, E. Philogéne, *J. Heterocycl. Chem.* **1983**, *20*, 1043 – 1046.
[49] M. Ikeda, K. Ohno, S. Mori, M. Takahashi, Y. Tamura, *J. Chem. Soc. Perkin Trans. 1* **1984**, 405 – 412.
[50] S. R. El-Ezbawy, A. M. A. Abdel-Wahab, *Phosphorus Sulfur Silicon Relat. Elem.* **1989**, *44*, 285 – 290.
[51] T. S. Wu, M. J. Liou, C. J. Lee, T. T. Jong, A. T. McPhail, *Tetrahedron Lett.* **1989**, *30*, 6649 – 6652.
[52] T. Gallagher, P. Magnus, *Tetrahedron* **1981**, *37*, 3889 – 3896.
[53] P. Marchand, M. Le Bogne, M. Duflos, S. Robert-Piessard, G. Le Baut, *Pharm. Pharmacol. Commun.* **1998**, *4*, 211 – 218.
[54] G. Galfré, S. C.Howe, C. Milstein, G. W. Butcher, J. C. Howard, *Nature* **1977**, *266*, 550 – 552.
[55] E. A. Guggenheim, *Phil. Mag.* **1926**, *2*, 538.

Received: November 29, 2002 [F4620]

